Soft Matter

PAPER

View Article Online
View Journal | View Issue

Cite this: *Soft Matter*, 2025, **21**, 6100

Hyperuniform mixing of binary active spinners†

Rui Liu, *[a] Mingcheng Yang [ab] and Ke Chen[ab]

Received 6th May 2025,
Accepted 4th July 2025

DOI: 10.1039/d5sm00458f

rsc.li/soft-matter-journal

Spinner mixtures consisting of both clockwise and counterclockwise self-spinning particles are often expected to phase separate. However, we demonstrate that such a demixing is absent for dimer (or rod-like) spinners. These particles always mix, even in a globally-hyperuniform way, with the total structure factor $S(q \to 0) \sim q^{\alpha}$ ($\alpha > 0$). This global hyperuniformity can be enhanced or weakened by changes in the driving torques or the particle density. The corresponding microscopic mechanism is attributed to the competition between a dynamical heterocoordination effect and effective like-particle attractions. Critical scaling for the absorbing state transition of the system is also found to persist, with a significant shift in its critical point observed. The system can be further thermalized, by the driving torques or through thermostating, into an ideal solution with identical partial radial distribution functions, which denies the possibility of being multi-hyperuniform. A simply-extended coupled density-oscillator theory explains why the system cannot be multi-hyperuniform, but can have a global hyperuniformity with the scaling exponent α approaching 2. Such a hyperuniform mixing provides a way to regulate the topological boundary flows of this chiral system, and this mixing regulation is found to barely affect the bulk density fluctuations, or even preserve the localization of the flows and the bulk hyperuniformity.

1. Introduction

Disordered hyperuniformity is an exotic property of matter, which indicates that the structure is isotropic as a liquid but suppresses long-wavelength density fluctuations as a crystal.[1–3] The concept has been extended to binary or multi-component systems, in which two-phase hyperuniformity,[4,5] global hyperuniformity[6] and multi-hyperuniformity[7,8] have been extensively investigated. Hyperuniformity properties are also known to persist in the active or fluidic states of single-component nonequilibrium/active systems.[9–12]

Binary or multi-component fluids may mix. Fluid mixing is a fundamental process in nature and industry, and a common problem in this process is whether a uniform mixture of different components can be obtained. External disturbing/driving, such as stirring, is usually employed to ensure that the liquid can be uniformly mixed. Active matter is driven by its internal energy sources, and thus would be usually more likely to mix. Whether or how hyperuniformity would persist for active fluidic mixtures remains to be explored. A recent study on a robot mixture with programmed nonreciprocal interactions[13] shows that hyperuniformity may exist at least in its critical absorbing state.

Active spinner systems, which consist of self-spinning particles, have been widely studied in recent years. They are known to exhibit a variety of interesting behaviors, such as phase separation,[14–16] jamming,[17] and topological effects.[18–21] Spinner mixtures consisting of both clockwise and counterclockwise self-spinning particles are often expected to phase separate. Even in purely repulsive systems, spinners with opposite rotation directions are found to segregate due to effective like-particle attractions,[14,15] and such a spin segregation may be even concomitant with a motility-induced phase separation.[22] For more complicated "wet" spinners, segregation can also be achieved.[16] Though there are cases that disc-shaped spinner mixtures driven by air do not phase separate[23,24] (probably due to the relatively weak tangential interactions between the particles), spin segregation is still anticipated to be observed as discussed in the earlier work.[23] Thus, spinner mixtures are generally expected to phase separate, especially for dry, purely-repulsive, and strongly-interacting systems. However, in this paper, we demonstrate that such a demixing behavior is absent for dry, repulsive dimer (or rod-like) spinners. These particles always mix, even in a hyperuniform way.

Through numerical simulations, we reveal that hyperuniformity typically persists in a global way for such a binary spinner fluid. The competition between dynamical heterocoordination and effective like-particle attraction can affect the long-wavelength scaling law of the total structure factor of the

[a] *Beijing National Laboratory for Condensed Matter Physics and CAS Key Laboratory of Soft Matter Physics, Institute of Physics, Chinese Academy of Sciences, Beijing 100190, China. E-mail: lr@iphy.ac.cn*
[b] *School of Physical Sciences, University of Chinese Academy of Sciences, Beijing 100049, China*

† Electronic supplementary information (ESI) available. See DOI: https://doi.org/10.1039/d5sm00458f

system. The heterocoordination effect may also cause a significant shift in the critical point of the absorbing state transition of the system. Subsequently, we show that increase in the driving torques may enhance the global hyperuniformity and that in density may somehow weaken it, leading to a collapsing long wavelength behavior in the total structure factor. Furthermore, the spinner mixture is shown to be thermalized into an ideal solution through either increasing the driving torque or particularly by thermostating.

Meanwhile, we extend the density oscillator model by Lei & Ni,[10] simply through introducing some linear couplings, to this binary system, which explains why the system cannot be multi-hyperuniform, but can have a global hyperuniformity with the scaling exponent α approaching 2. As a potential application, we further show that such a mixing can provide an intriguing way to regulate the robust topological boundary flows of such chiral active fluids, which preserves localization of the flows and hyperuniformity properties in the bulk.

2. Simulation and theory

We simulate a two-dimensional (2D) active spinner system as that in our previous study.[11] Each spinner is a dimer consisting of two spherical monomers bonded with a fixed length $\sigma = 1$. Each monomer has a mass $m = 1$ and each dimer has a moment of inertia $I = \frac{1}{2}m\sigma^2$. The monomers from different dimers interact with each other through a Weeks–Chandler–Andersen potential $U(r_{ij}) = 4\hat{\varepsilon}\left[\left(\frac{\sigma}{r_{ij}}\right)^6 - \left(\frac{\sigma}{r_{ij}}\right)^{12}\right] + \hat{\varepsilon}$, when their separation r_{ij} is smaller than a cutoff distance $r_c \equiv 2^{1/6}\sigma$. With the total effect of all such pair interactions denoted by $U(t)$, the dynamics of any dimer i is governed by

$$2m\ddot{\mathbf{r}}_i = -2\gamma_t\dot{\mathbf{r}}_i - \nabla_i U(t) + \boldsymbol{\xi}_i(t), \quad (1)$$

$$I\ddot{\theta}_i = \pm\tau - \gamma_s\dot{\theta}_i - \partial_{\theta_i}U(t) + \zeta_i(t). \quad (2)$$

Assuming $\hat{\varepsilon} = 1$ energy unit, and taking $\hat{t} = \sqrt{m\sigma^2/\hat{\varepsilon}}$ to be the time unit, we always set the translational frictional coefficient $\gamma_t = m/\hat{t}$ and the rotational counterpart $\gamma_s = I/\hat{t}$ in our simulation. The driving torques $\pm\tau$ are respectively applied to make the dimers spin in the counterclockwise and clockwise directions (a percentage composition of 50 : 50 is usually adopted, if not specified). $\boldsymbol{\xi}_i(t)$ and $\zeta(t)$ are respectively the stochastic force and torque due to thermal fluctuations: $\langle\boldsymbol{\xi}_i(t)\boldsymbol{\xi}_j(t')\rangle = 2\gamma_t k_B T\delta_{ij}\delta(t-t')$, $\langle\zeta_i(t)\zeta_j(t')\rangle = 2\gamma_s k_B T\delta_{ij}\delta(t-t')$. The timestep of the simulation is adjusted accordingly for different driving torques and thermostating temperatures.

Typically, a system with N dimers in a square box of size L is simulated, and the number density is evaluated as $\rho = N/L^2$, or $\phi = N\sigma^2/L^2$ in a dimensionless way. Periodic boundary conditions are applied for all the box boundaries. Similar measurements are adopted for the system simulated in a disc container to demonstrate the regulation of topological boundary flows, where a smooth spherical wall is used to confine the system. All simulations run for no less than 3×10^7 time steps, to ensure the system reaches a steady state and good statistical results can be obtained.

The dimers are driven through torques acting on each monomer, which thus preserve the center-of-mass conservation (COMC). COMC is crucial for density hyperuniformity,[9,25] and this provides a general explanation as to why spinner systems possess hyperuniform properties in various manners.[10,11,26] By neglecting the spin–orbit coupling, and encoding the driving effect into the kinetic temperature T_k, a generic density oscillator theory for such active fluids is given by Lei & Ni[10] (see also Section V in the ESI† for a brief review):

$$\frac{\partial^2\delta\rho_q}{\partial t^2} = -\Gamma_q\frac{\partial\delta\rho_q}{\partial t} - Dq^2\delta\rho_q + q^2\sigma^r + q\sigma^t, \quad (3)$$

where $\delta\rho$ is the density fluctuation, q is the modulus of the wave vector $\mathbf{q}$, Γ_q describes the total effect of both the substrate friction and kinematic viscosities, D describes the diffusional effect, and σ^r denotes the longitudinal term of the collisional noise. Transverse modes are ignored since they are irrelevant to the density fluctuations. Additionally, a longitudinal thermal noise term σ^t is added here.

A simple extension to the binary system would be assuming linear coupling between the density fluctuations of the two species: $\delta\rho = (\delta\rho_1, \delta\rho_2)^T$. Thus the dynamical coefficients Γ_q and D become matrices:

$$\Gamma_q = \begin{bmatrix} \gamma+\eta q^2 & \chi \\ \chi & \gamma+\eta q^2 \end{bmatrix}, \quad D = \begin{bmatrix} c_s^2 & \beta \\ \beta & c_s^2 \end{bmatrix}, \quad (4)$$

where $\gamma = \gamma_t/m$ is the reduced frictional coefficient, η is the longitudinal viscosity, c_s is the sound speed, χ describes the inter-species momentum transfer as a frictional term, and β measures the effect of inter-species pressure on diffusion.

Obviously, each species by itself does not preserve COMC. Thus the collisional noise σ^r cannot be naively decomposed into two surface terms. We assume, for each species, that the noise can be decomposed into a gradient term and an ordinary thermal-like noise. Thus we have

$$q^2\sigma^r \to (q^2\sigma_1^r + \mathbf{q}\cdot\delta\sigma^r,\ q^2\sigma_2^r - \mathbf{q}\cdot\delta\sigma^r)^T. \quad (5)$$

In this way, we have the separated COMC terms of collisional noises $\tilde{\sigma}^r = (\sigma_1^r, \sigma_2^r)^T$ and effective longitudinal thermal noises $\tilde{\sigma}^t = (\sigma_1^t + \delta\sigma^r,\ \sigma_2^t - \delta\sigma^r)^T \equiv (\sigma_1^t + \delta\sigma_1^r,\ \sigma_2^t + \delta\sigma_2^r)^T$. By performing a temporal Fourier transform, eqn (3) can be rewritten as:

$$(-\omega^2 I - i\omega\Gamma_q + Dq^2)\delta\rho(q,\omega) = q^2\tilde{\sigma}^r + q\tilde{\sigma}^t. \quad (6)$$

Assuming that all random terms are both spatially and temporally white: $\left\langle\sigma_\mu^r\sigma_\nu^r\right\rangle(\mathbf{q},\omega) = a(T_k)\rho\sqrt{x_\mu x_\nu}\delta_{\mu\nu}$, $\left\langle\delta\sigma_\mu^r\delta\sigma_\nu^r\right\rangle(\mathbf{q},\omega) = b(T_k)\rho\sqrt{x_\mu x_\nu}\varepsilon_{\mu\nu}$, and $\left\langle\sigma_\mu^t\sigma_\nu^t\right\rangle(\mathbf{q},\omega) = c(T)\rho\sqrt{x_\mu x_\nu}\delta_{\mu\nu}$ ($x_{\mu,\nu}$ are respectively the concentrations of species μ and ν; T is the temperature of the thermostat and the driven system has a non-zero kinetic temperature T_k even at $T = 0$; $\varepsilon_{\mu\nu} = 1$ for $\mu = \nu$, and -1

for $\mu \neq \nu$), one obtains the following results for an equimolar system ($x_1 = x_2 = 1/2$):

$$\begin{aligned} S_{\mu,\nu}(q,\omega) &= \left\langle \delta\rho_\mu \delta\rho_\nu^* \right\rangle \\ &= \sum_{\kappa\lambda} M_{\mu\kappa} M_{\nu\lambda}^* \left[q^4 \left\langle \sigma_\kappa^{\mathrm{r}} \sigma_\lambda^{\mathrm{r}} \right\rangle + q^2 \left\langle \tilde{\sigma}_\kappa^{\mathrm{t}} \tilde{\sigma}_\lambda^{\mathrm{t}} \right\rangle \right] \\ &= \frac{1}{2}(aq^4 + cq^2)\rho \sum_\lambda M_{\mu\lambda} M_{\nu\lambda}^* + \frac{1}{2} bq^2 \rho \sum_{\kappa\lambda} M_{\mu\kappa} M_{\nu\lambda}^* \varepsilon_{\kappa\lambda}, \end{aligned}$$

where $\langle\cdot\rangle$ denotes an ensemble average, and $M = (-\omega^2 I - i\omega\Gamma_{\mathrm{q}} + Dq^2)^{-1}$. Due to the symmetry of M, all calculation results will reduce to matrix elements of $K = MM^*$:

$$\begin{aligned} S_{11}(q,\omega) &= S_{22}(q,\omega) \\ &= \frac{\rho}{2}\left[(aq^4 + cq^2) K_{11} + bq^2 (K_{11} - K_{12}) \right], \\ S_{12}(q,\omega) &= S_{21}(q,\omega) \\ &= \frac{\rho}{2}\left[(aq^4 + cq^2) K_{12} - bq^2 (K_{11} - K_{12}) \right]. \end{aligned}$$

Then the total structure factor is given by:

$$\begin{aligned} S(q,\omega) &= \sum_{\mu\nu} S_{\mu\nu}(q,\omega) \\ &= \rho (aq^4 + cq^2)(K_{11} + K_{12}). \end{aligned}$$

The bq^2 terms simply cancel out, and the cq^2 terms will not be present for the case without thermal noise. By integrating with ω, one obtains:

$$\int_{-\infty}^{\infty} (K_{11} \pm K_{12}) \mathrm{d}\omega = \frac{\pi}{q^2 (c_{\mathrm{s}}^2 \pm \beta)(\gamma + \eta q^2 \pm \chi)}.$$

For $T = 0$, we simply have $S(q \to 0) \sim q^2$:

$$S(q) = \int_{-\infty}^{\infty} S(q,\omega) \mathrm{d}\omega = \frac{\pi \rho a q^2}{(c_{\mathrm{s}}^2 + \beta)(\gamma + \eta q^2 + \chi)}. \tag{7}$$

Thus, theoretically, hyperuniformity may persist in such a binary fluid, keeping the scaling exponent $\alpha = 2$. However, the inter-species and inner-species spinner–spinner interactions are generally different, and thus there is pairing noise which causes local concentration fluctuations. The pairing noise preserves COMC only globally, but not locally. This may lead to q-dependencies in the above correlation functions of the random terms, which would further cause a decrease in the scaling exponent α. Thus a weaker hyperuniformity characterized by a smaller α is acceptable (see Section VI in the ESI† for more explanation).

One may expect the binary system to be multi-hyperuniform. However, we have $S_{11} \sim aq^2 + b$ with a nonvanishing q-independent term b, which indicates that the subsystem constituted by one of the two species is inevitably non-hyperuniform. Thus, we do not have a multi-hyperuniformity in general. Nevertheless, the global hyperuniformity with a scaling exponent α approaching 2 can still be expected.

3. Dynamical heterocoordination and global hyperuniformity

Numerically, we first investigate such a spinner system without thermal noise, *i.e.* $T = 0$. Fig. 1 shows our simulation results of the system at different densities. We observe an effective unlike-particle attraction for all the cases: the cross terms $g_{\mu\nu}(r)$ ($\mu \neq \nu$) of the partial radial distribution functions surpass the diagonal terms $g_{\mu\mu}(r)$ ($\mu = 1, 2$) just before/at the major peak, as shown in Fig. 1(a). This is similar to that of the negatively-nonadditive hard-disk plasmas,[6] which show a heterocoordination effect and do not have a demixing transition. These effects are demonstrated to be compatible with a global hyperuniformity for the binary mixture.

Demixing is also found to be absent here for our dimer (or generically rod-like) spinners, and we expect a similar global hyperuniformity to be observed as that in negatively-nonadditive hard-disk plasmas. We calculate the total structure factor[6,8] for this system:

$$\begin{aligned} S(q) &= 1 + \rho \sum_{\mu\nu} x_\mu x_\nu \mathscr{F}\left[g_{\mu\nu}(r) - 1 \right](q) \\ &= 1 + \rho \sum_{\mu\nu} x_\mu x_\nu h_{\mu\nu}(q) \end{aligned} \tag{8}$$

where $\mathscr{F}[\cdot]$ represents a Fourier transform, $h(q) \equiv \mathscr{F}[h(r)](q) = \mathscr{F}[g(r) - 1](q)$. The corresponding results are shown in Fig. 1(b).

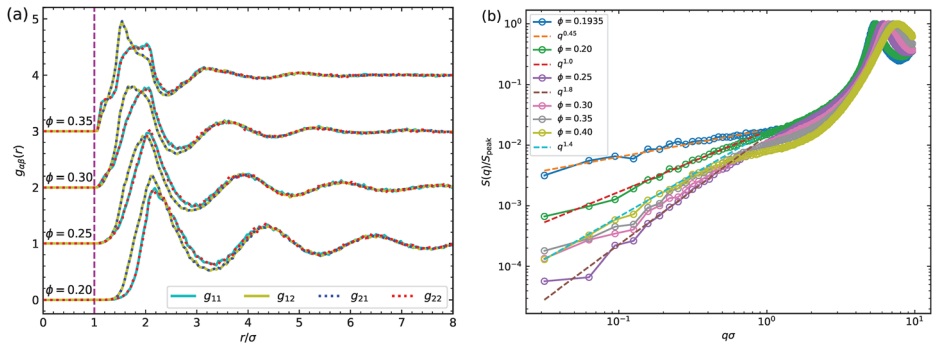

Fig. 1 The binary active spinner system at $\tau = 1$, $T = 0$, $L = 200\sigma$, and varying $\phi = 0.20, 0.25, 0.30, 0.35$: (a) partial radial distribution functions $g_{\mu\nu}(r)$ (vertically shifted by 1 for each ϕ, which is adopted below without further explanations); (b) the total structure factor, with $S(q \to 0) \sim q^{\alpha}$.

Generally, we have the power-law scaling in the total structure factor $S(q \to 0) \sim q^{\alpha}$ with $\alpha \gtrsim 1$ for all $\phi \geq 0.20$, which indicates a strong global hyperuniformity for all densities in the active fluidic regime. The system stays in an absorbing state below $\phi_c \approx 0.19$ [which has the critical scaling exponent $\alpha_c \approx 0.45$ as shown in Fig. 1(b)], and becomes a mixed active fluid above this critical point (see Sections I & II in the ESI† for more details on the transition). Compared with Lei & Ni's result that $\phi_c < 0.15$,[10] we have an observable shift in the critical density, due to the dynamical heterocoordination effect. Another significant difference in this binary system is that it does not exhibit the same scaling $S(q) \sim q^2$ beyond the critical point, *i.e.* in the active state, which holds for single-component systems.[9,10]

We have a maximum exponent $\alpha \approx 1.8$ at about $\phi = 0.25$, which is close to the value $\alpha = 2$ for single-component spinners. We assume that this corresponds to the predicted results $S(q) \sim q^2$ in the theory section. The exponent first increases from the critical value 0.45 to 1.8 and then decreases to a relatively lower value $\alpha = 1.4$, as the density increases, giving a varying scaling law at long wavelengths. We argue that the varying scaling law and the deviation from $\alpha = 2$ are due to the competition between dynamical heterocoordination and some effective like-particle attraction. We observe that for a denser system at $\phi = 0.35$, $g_{11}(r)$ becomes higher than $g_{12}(r)$ just before the major peak [Fig. 1(a)], which may indicate an effective like-particle attraction. The dynamical heterocoordination effect is likely to enhance mixing, while the effective like-particle attraction tries to induce a phase separation. The competition between these two effects causes the so-called pairing noise, which does not preserve COMC locally. Thus, one observes such a non-monotonic change in the scaling exponent α.

Previously, the effective like-particle attractions are adopted to explain how binary spinners phase separate.[14,15] The microscopic picture for such an attraction is depicted as: pairs of like particles stay together relatively longer than unlike-particle pairs during collisions. However, for the dimmer or rod-shaped spinners here, we argue that like pairs have large relative tangential velocities during collisions, and a system minimizing its dissipation would avoid like pairing in its steady state. Or equivalently, unlike dimers with proper phase differences can stay closer into each other's sweeping range (see Fig. S5 in Section IV of the ESI†), which can be effectively treated as an attraction. All these effects are subtle. What favors unlike pairing may be roughly compensated by what else favors like pairing. This may finally lead to an ideal mixing with identical radial distribution functions for the two species (see below).

4. Enhanced hyperuniformity and self-thermalization

The driving torques of the spinners would enhance the global hyperuniformity at low densities. An apparent example would be the system at density $\phi = 0.15$, as shown in Fig. 2. At $\tau = 1$, the system is below the critical point of the absorbing state transition, which is thus intrinsically non-hyperuniform. However it becomes strongly hyperuniform with the scaling exponent $\alpha \gtrsim 1.5$ at $\tau = 5$, as shown in Fig. 2(b). The critical density of the transition decreases to an even lower value $\phi_c \approx 0.099$ [the data with $q^{0.45}$ scaling as a guide for the eye in Fig. 1(b)]. For the system at $\phi = 0.2$, which is in the active state for both $\tau = 1$ and 5, a significant promotion in the scaling exponent α from the critical value 0.45 to about 1.5 is also observed, compared with the data shown in Fig. 1(b).

However, for larger densities, high torques seem to be not beneficial to hyperuniformity. As can be seen from Fig. 2(b), the scaling exponent α for $\phi = 0.35$ or 0.4 is just about 1.2, which is lower than that of $\phi = 0.2$, or even the corresponding value of its own at $\tau = 1$ in Fig. 1(b). This weakening in hyperuniformity is due to the effective like-particle attraction, identified by $g_{11}(r) > g_{12}(r)$ just beyond $r = 1\sigma$ as shown in Fig. 2(a). This effect dominates only at nearer separations of the spinners, which thus usually require a larger density for the system.

Moreover, high torques seem to make the long wavelength (small q) behaviors of $S(q)$ at different ϕ collapse, but distinguish the density differences in the intermediate range of q. The scaling exponent increases rapidly from the critical value $\alpha_c = 0.45$ to about 1.5 (see Section III in the ESI†for more data in between), and stays in roughly the range (1.2, 1.5) for a wide range of densities $\phi \gtrsim 0.15$, as shown in Fig. 2(b). The collapse

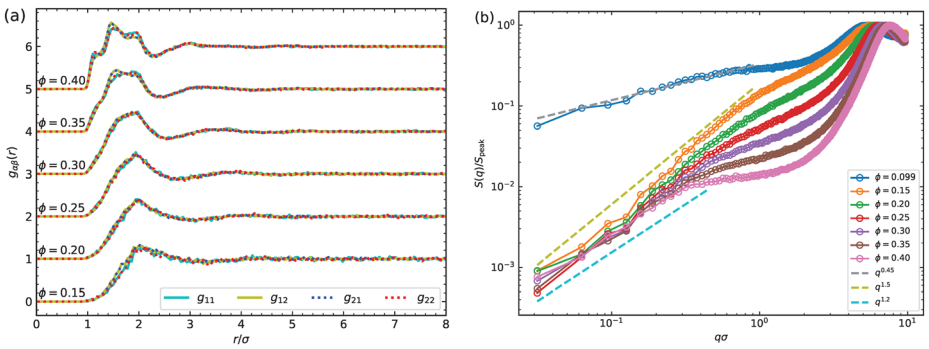

Fig. 2 The binary active spinner system at $\tau = 5$, $T = 0$, $L = 200\sigma$: (a) The partial radial distribution functions $g_{\mu\nu}(r)$; (b) the total structure factor $S(q)$; dashed lines show some asymptotic scalings at long wavelengths.

is due to the joint effect of torque-enhancing and density-weakening effects mentioned above. The intermediate range at the order of $q\sigma \sim 1$ corresponds to the length scale of spinner–spinner interactions, and structures at these length scales may be significantly changed by the driving torques.

Accompanied with the enhancement of hyperuniformity, we observe an identification of all partial radial distribution functions $g_{\mu\nu}(r)$ of the system, for densities $\phi < 0.35$ [Fig. 2(a)]. All $g_{\mu\nu}(r)$ become more and more identical as the density increases from 0.15 to 0.30. This is obviously due to the increased probability of spinner–spinner interactions. Larger torques would heat the system up more easily and thus also enhance the spinner–spinner interactions. Identical partial radial distributions correspond to an ideal solution described by the substitutional model of Faber & Ziman,[27] which has a constant concentration–concentration structure factor $S_{cc}(q)$. Thus, the system cannot be multi-hyperuniform, which requires both vanishing $S(q)$ and $S_{cc}(q)$ as q approaches zero. However, the system can still be globally hyperuniform as discussed above, since we do not introduce any thermal noise ($T = 0$), which does not abide by COMC. The current thermalization only causes a slight decrease in the scaling exponent α, as the density increases. Since such a thermalization is much easier to be achieved in the presence of thermal noise, we will discuss it further below.

5. Thermalization and ideal solution

Thermal noise is known to weaken or destroy hyperuniformities.[28] We also investigate the thermal effects on the global hyperuniformity of this binary mixture. We observe a notable thermalization characteristic for a wide range of densities:

$$g_{11}(r) = g_{22}(r) = g_{12}(r) = g_{21}(r). \quad (9)$$

Namely, we have again identical partial radial distribution functions [as shown in Fig. 3(a)], which correspond to an ideal solution with constant concentration–concentration fluctuations[6,8,29] at all modes, *i.e.*:

$$S_{cc}(q) = x_1x_2\left[1 + \rho x_1x_2\sum_{\mu\nu}\varepsilon_{\mu\nu}h_{\mu\nu}(q)\right] = x_1x_2. \quad (10)$$

For an equimolar binary system, one has $S_{cc}(q) = 0.25$.

Thus, as mentioned above, there is no chance for the system to become multi-hyperuniform. We still calculate the total structure factor $S(q)$ for the system, which is shown in Fig. 3(b). We have a robust scaling relation $S(q) \sim q^{0.08}$ at small q, though the constant exponent is rather small. This could be the remnant of the above non-thermal hyperuniformity, and one may conclude that such a thermalized system is rather weakly hyperuniform or just nonhyperuniform in the global sense.

However, we still observe a drastic decrease in $S(q \to 0)$ as the density of the system increases. This is due to the fact that the system starts to pack for increased density. Such a packing effect would lead to a jamming-type hyperuniformity[30,31] or spinners' nonhyperuniformity with lowly-confined density fluctuations.[11] In either case, the long-wavelength behavior $S(q \to 0)$ should be decreased, as has been observed.

6. Preserved hyperuniformity in mixing regulation

The chiral system of single-component spinners is known to exhibit robust topological boundary flows.[18,19] Usually, it would be a challenge to regulate such a flow without altering the corresponding carrier density. Since binary spinners can mix hyperuniformly, we may utilize such a feature to tune the topological boundary flow by simply adjusting the concentrations of the two species in the system.[32] Such a regulation would be preferable in experimental systems, especially for sealed samples where the density of particles can be hardly changed.

Here, we focus on the regulation effect on the density fluctuations in the bulk. Fig. 4(a) shows the total structure factor $S(q)$ corresponding to a system with weakly-localized boundary flows in a disc of size $R = 100\sigma$, where the flow profile extends to the center of the disc (see the inset). The measurement of $S(q)$ is performed in a square subarea of size $L_s = 0.8R$ at the center of the disc. The subsystem does not preserve COMC globally, due to the in- and out-flows of particles. For the existence of the obvious flow, the whole system possesses no obvious hyperuniformity features. While the regulation is effective for the whole flow field, we observe a preservation in the

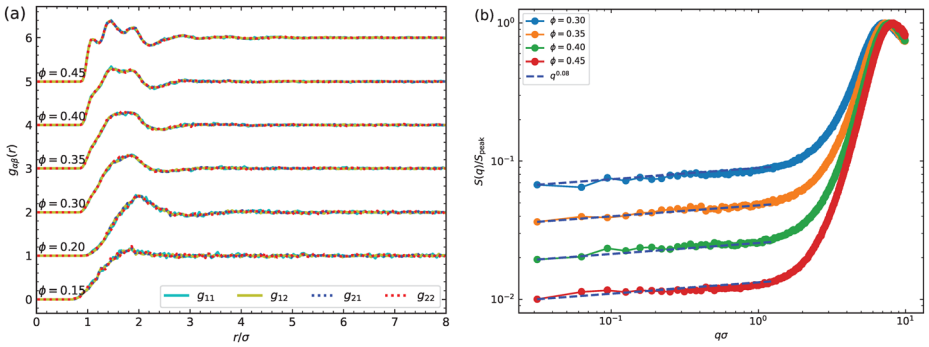

Fig. 3 Thermalization of the binary spinner system at $\tau = 1$, $T = 1$, $L = 200\sigma$: (a) Identical partial radial distribution functions $g_{\mu\nu}(r)$ at various densities; (b) the total structure factor $S(q)$, with a drastic decrease in $S(q \to 0)$ as the density increases; dashed lines show a $q^{0.08}$ scaling.

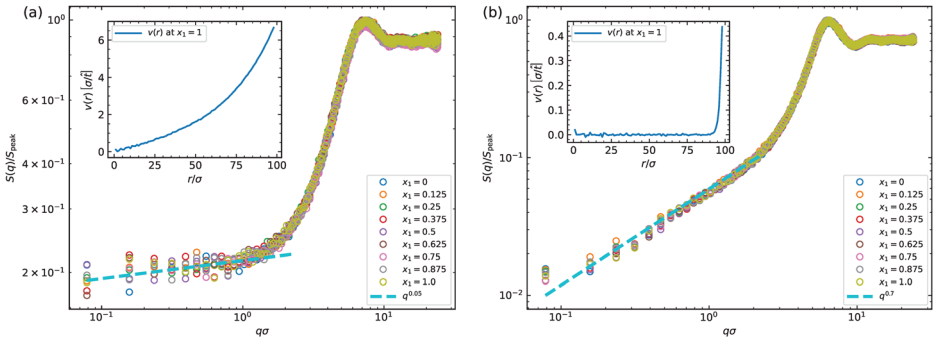

Fig. 4 Binary spinners in a disc of radius $R = 100\sigma$ simulated with $T = 0$, $\tau = 5$, $\phi \approx 0.255$: (a) nearly collapsed total structure factor $S(q)$ for various x_1 in the presence of weakly-localized boundary flows; the inset plots the radial flow profile $v(r)$ at $x_1 = 1$; (b) nearly collapsed total structure factor $S(q)$ for various x_1 in the presence of strongly-localized boundary flows; the inset plots the flow profile at $x_1 = 1$. All $S(q)$ measurements are performed in a centered square subarea of size $L_s = 0.8R$.

density fluctuations of the bulk: the total structure factor $S(q)$ is nearly collapsed for different concentrations in the full range [0,1], which indicates that the density fluctuations in the bulk are not significantly altered by the regulation.

When the topological boundary flow is strongly localized, with an inner zero velocity field, the regulation will only affect the boundary flow, and abides by localization. No obvious flow in the bulk admits a global hyperuniformity of the mixture, though COMC is not globally preserved. In Fig. 4(b), we show the total structure factor $S(q)$ for the same system with a strongly localized boundary flow (see the inset). The total structure factor is again nearly collapsed for different concentrations in the full range [0,1], but accompanied by an obvious hyperuniformity feature $S(q \to 0) \sim q^{0.7}$. Hence, the mixing regulation will also preserve localization and hyperuniformity properties. Though the mixing preservation of localization and global hyperuniformity is more notable, the fact that such a regulation barely affects the density fluctuations in the bulk is more general, which holds for even the non-hyperuniform cases.

7. Conclusions

In conclusion, we show that demixing is absent for binary dimer (or rod-like) spinner mixtures due to a dynamical hetero-coordination effect. Global hyperuniformity is also found to persist in this kind of mixed fluid, and can be enhanced or weakened by torques or densities in various ways. Correspondingly, a long wavelength scaling law $S(q \to 0) \sim q^{\alpha}$ $(\alpha > 0)$ exists in the total structure factor of the system, where the exponent reaches a maximum value of about 1.8 at around $\phi = 0.25$. The deviation in the exponent from the theoretical value 2 and the variation of the long-wavelength scaling law are attributed to the results of pairing noises, *i.e.* the competition between the dynamical heterocoordination effect and the effective like-particle attractions. The absorbing state transition with the critical scaling $S(q) \sim q^{0.45}$ is observed as well for this binary system, and the corresponding critical point is found to shift to an obviously higher density. When heated up by the driving torques of the spinners or through thermostating, the binary system exhibits a notable feature that all partial radial distribution functions become identical. This leads to a constant concentration–concentration structure factor, which prevents the system from being multi-hyperuniform.

As a potential application, such a hyperuniform mixing is further shown to be beneficial to the regulation of robust topological boundary flows. The great advantage of this mixing regulation, that it barely affects the bulk density fluctuations even in a non-uniform flow field, is rather intriguing. The regulation method also shows its delicacy in preserving localization and bulk hyperuniformity for systems with strongly-localized boundary flows. Experiments on rotors driven by light or electric/magnetic fields[12,33] may hopefully verify our results.

Conflicts of interest

There are no conflicts to declare.

Data availability

The data that support the findings of this study are available from the corresponding author upon reasonable request.

Acknowledgements

We are extremely grateful to Ran Ni for helpful discussions and comments. This work is supported by the National Natural Science Foundation of China (Grant No. T2325027, 11774393 and 11404378) and Youth Innovation Promotion Association of CAS (No. 2017014).

Notes and references

1 S. Torquato, *Phys. Rep.*, 2018, **745**, 1–95.
2 S. Torquato and F. H. Stillinger, *Phys. Rev. E*, 2003, **68**, 041113.
3 S. Torquato, *Phys. Rev. E*, 2016, **94**, 022122.
4 D. Chen and S. Torquato, *Acta Mater.*, 2018, **142**, 152–161.

5 Z. Ma, E. Lomba and S. Torquato, *Phys. Rev. Lett.*, 2020, **125**, 068002.
6 E. Lomba, J. J. Weis and S. Torquato, *Phys. Rev. E*, 2017, **96**, 062126.
7 Y. Jiao, T. Lau, H. Hatzikirou, M. Meyer-Hermann, C. C. Joseph and S. Torquato, *Phys. Rev. E*, 2014, **89**, 022721.
8 E. Lomba, J. J. Weis and S. Torquato, *Phys. Rev. E*, 2018, **97**, 010102.
9 D. Hexner and D. Levine, *Phys. Rev. Lett.*, 2017, **118**, 020601.
10 Q. L. Lei and R. Ni, *Proc. Natl. Acad. Sci. U. S. A.*, 2019, **116**, 22983–22989.
11 R. Liu, J. Gong, M. Yang and K. Chen, *Chin. Phys. Lett.*, 2023, **40**, 126402.
12 B. Zhang and A. Snezhko, *Phys. Rev. Lett.*, 2022, **128**, 218002.
13 J. Chen, X. Lei, Y. Xiang, M. Duan, X. Peng and H. P. Zhang, *Phys. Rev. Lett.*, 2024, **132**, 118301.
14 N. H. P. Nguyen, D. Klotsa, M. Engel and S. C. Glotzer, *Phys. Rev. Lett.*, 2014, **112**, 075701.
15 C. Scholz, M. Engel and T. Poschel, *Nat. Commun.*, 2018, **9**, 931.
16 K. Yeo, E. Lushi and P. M. Vlahovska, *Phys. Rev. Lett.*, 2015, **114**, 188301.
17 B. C. van Zuiden, J. Paulose, W. T. Irvine, D. Bartolo and V. Vitelli, *Proc. Natl. Acad. Sci. U. S. A.*, 2016, **113**, 12919–12924.
18 K. Dasbiswas, K. K. Mandadapu and S. Vaikuntanathan, *Proc. Natl. Acad. Sci. U. S. A.*, 2018, **115**, E9031–E9040.
19 A. Souslov, K. Dasbiswas, M. Fruchart, S. Vaikuntanathan and V. Vitelli, *Phys. Rev. Lett.*, 2019, **122**, 128001.
20 Q. Yang, H. Zhu, P. Liu, R. Liu, Q. Shi, K. Chen, N. Zheng, F. Ye and M. Yang, *Phys. Rev. Lett.*, 2021, **126**, 198001.
21 P. Liu, H. Zhu, Y. Zeng, G. Du, L. Ning, D. Wang, K. Chen, Y. Lu, N. Zheng, F. Ye and M. Yang, *Proc. Natl. Acad. Sci. U. S. A.*, 2020, **117**, 11901–11907.
22 B.-Q. Ai, S. Quan and F.-G. Li, *New J. Phys.*, 2023, **25**, 063025.
23 S. Farhadi, S. Machaca, J. Aird, B. O. T. Maldonado, S. Davis, P. E. Arratia and D. J. Durian, *Soft Matter*, 2018, **14**, 5588–5594.
24 M. A. Lopez-Castano, A. Rodriguez-Rivas and F. V. Reyes, *Front. Phys.*, 2022, **10**, 972051.
25 F. D. Luca, X. Ma, C. Nardini and M. E. Cates, *J. Phys.: Condens. Matter*, 2024, **36**, 405101.
26 Y. Lei and R. Ni, *J. Phys.: Condens. Matter*, 2025, **37**, 023004.
27 T. E. Faber and J. M. Ziman, *Philos. Mag.*, 1965, **11**, 153–173.
28 Q. L. Lei, M. P. Ciamarra and R. Ni, *Sci. Adv.*, 2019, **5**, eaau7423.
29 A. B. Bhatia and D. E. Thornton, *Phys. Rev. B: Condens. Matter Mater. Phys.*, 1970, **2**, 3004–3012.
30 C. E. Zachary, Y. Jiao and S. Torquato, *Phys. Rev. E*, 2011, **83**, 051308.
31 D. Hexner, A. J. Liu and S. R. Nagel, *Phys. Rev. Lett.*, 2018, **121**, 115501.
32 The related results will be published elsewhere.
33 Y. Zong, J. Liu, R. Liu, H. Guo, M. Yang, Z. Li and K. Chen, *ACS Nano*, 2015, **9**, 10844–10851.

